

# Structural and dielectric properties of epitaxial SrTiO<sub>3</sub> films grown directly on GaAs substrates by laser molecular beam epitaxy

Z. P. Wu, W. Huang,<sup>a)</sup> K. H. Wong, and J. H. Hao<sup>b)</sup>

Department of Applied Physics, The Hong Kong Polytechnic University, Hong Kong, People's Republic of China

(Received 17 March 2008; accepted 28 June 2008; published online 4 September 2008)

Epitaxial SrTiO<sub>3</sub> films were grown on GaAs (001) substrates without any buffer layers using laser molecular beam epitaxy technique. The reflection high-energy electron diffraction observations have revealed that a layer-by-layer growth of SrTiO<sub>3</sub> was achieved at optimized deposition conditions. The crystalline orientation of the as-grown SrTiO<sub>3</sub> (001) films rotates 45° in plane with respect to the GaAs substrates. Atomic force microscope studies show that these films possess atomically flat surfaces. The dielectric properties of the heterostructure were also investigated. Our results have clearly demonstrated the practicality of integrating perovskite oxide thin films with GaAs substrates. © 2008 American Institute of Physics. [DOI: [10.1063/1.2974796](https://doi.org/10.1063/1.2974796)]

## I. INTRODUCTION

Integration of functional oxide thin films with semiconductors has attracted considerable attention in recent years.<sup>1,2</sup> For instance, SrTiO<sub>3</sub> (STO) which is an incipient ferroelectric material having a large and variable dielectric constant, has been intensely studied for applications in tunable microwave devices.<sup>3,4</sup> STO also possesses a cubic perovskite structure and has a lattice closely matched with a large number of functional perovskite materials.<sup>5,6</sup> These characteristics thus make STO a suitable template for growth of high quality functional thin films. Recently, the epitaxial growth of STO on Si has been studied extensively. The integration of STO with Si has shown desirable interfacial structural and electronic properties.<sup>7-9</sup> Compared to Si, GaAs with a zincblende structure and a higher saturated electron mobility is the new generation semiconductor.<sup>10</sup> Transistors based on GaAs could function at much higher frequencies. Also, GaAs has a direct band gap. When combined with STO, it can offer superior optical and electronic properties.<sup>11</sup> Additional magneto-optical and electro-optical functionalities can also be incorporated through integration of magnetic and electro-optic oxides with the STO/GaAs heterostructure. In order to get low interface defect and better electronic property, high quality single-crystal film is required. Unfortunately, the successful epitaxial growth of STO thin film on GaAs is difficult due to structural incompatibility and interdiffusion between GaAs and STO. So far, epitaxial thin film of STO grown on GaAs has only been achieved via a complex molecular beam epitaxy with a submonolayer of titanium as buffer.<sup>11,12</sup> In this work, we report on using a relatively simple and stoichiometric fabrication method, laser molecular beam epitaxy (LMBE), to fabricate high-quality single crystal STO thin

films on GaAs without buffer layers. Studies of the microstructure and dielectric properties of these STO/GaAs heteroepitaxial structures are also presented.

## II. EXPERIMENT

Thin films of STO were deposited directly on GaAs (001) substrates by LMBE. As the surface oxides can desorb at about 600 °C, the GaAs wafer was first *in situ* heated up to 650 °C in vacuum for 2 min to remove the native oxide layer. A single-crystalline STO target was ablated using a KrF excimer laser of 248 nm wavelength with an energy density of 6 J/cm<sup>2</sup>. The target was rotated during the deposition process to reduce nonuniform ablation. The substrate was placed parallel to the target at a distance of 6 cm. The growth rate of STO was about 0.03 nm/pulse. During the deposition, the chamber was evacuated to a base pressure of 5 × 10<sup>-5</sup> Pa to avoid oxidation of the GaAs substrate; the substrate temperature was kept at about 600 °C. The deposited films were then *in situ* annealed at 420 °C in ambient of high oxygen pressure for a few hours before being cooled down to room temperature. This was to ensure oxygen stoichiometry in the STO films. A reflective high energy electron diffraction (RHEED) system with an incident energy of 30 kV and an incident angle of about 2.5° was used to monitor the film growth process. In order to study the dielectric properties of the STO/GaAs heterojunction, Pt spot electrodes with a diameter of about 0.2 mm were fabricated on the top. *P*-type GaAs was used as a bottom electrode in our study. The resistivity of used GaAs wafer was estimated to be 2~6 Ω cm. Electrical properties of the STO films were investigated using a Hewlett Packard 4294A LCR meter.

## III. RESULTS AND DISCUSSIONS

Figure 1 is the RHEED patterns showing the epitaxial features of the STO film grown on GaAs substrate. In comparison with GaAs zincblende structure crystal, the STO has a perovskite cubic structure at room temperature. Both GaAs (face-centered cubic  $a=0.56$  nm) and STO (primitive cubic

<sup>a)</sup>Also at State Key Laboratory of Electronic Thin Films and Integrated Devices, University of Electronics Science and Technology of China, Chengdu, People's Republic of China.

<sup>b)</sup>Author to whom correspondence should be addressed. Electronic mail: [apjhao@polyu.edu.hk](mailto:apjhao@polyu.edu.hk).

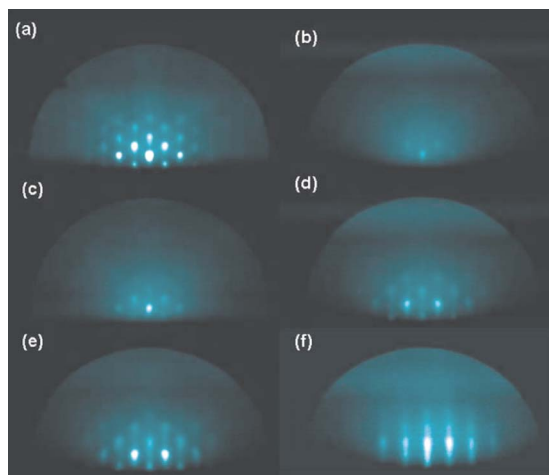


FIG. 1. (Color online) The RHEED diffraction patterns recorded as a function of film thickness during the process of STO growth, (a) 0 nm, (b) 0.5 nm, (c) 1 nm, (d) 2 nm, (e) 3 nm, and (f) 300 nm.

$a=0.3905$  nm) exhibit a cubic symmetry. Thus, the lattice mismatch between STO and GaAs is relatively large at about 31%. However, according to RHEED patterns in Fig. 1, good epitaxial nature of STO film on a single crystal *p*-GaAs substrate could be observed. At the initial growth stage of GaAs film, the laser repetition was programmed to 1 Hz. The diffraction spots of GaAs representing (200) plane cluster in the RHEED pattern [seen in Fig. 1(a)] gradually disappeared [seen in Figs. 1(b) and 1(c)]. Then two elongated bright spots emerged with a wider separation [seen in Fig. 1(d)]. According to the Bragg's diffraction law, epitaxial STO film starts to grow with an in-plane rotation. The spotty diffraction pattern in Fig. 1(e) indicates that the interface at the first few atomic layers is not quite smooth. At subsequent growth the film thickness was increased. Conspicuous streaky diffraction patterns of the (001) plane of STO could be observed in Fig. 1(f). This suggests that the growth becomes a two dimensional layer-by-layer mode as the STO film thickens. During the whole growth process, no unidentifiable RHEED patterns were detected. Apparently no other unstable phases existed despite the complex stoichiometry of titanium oxide. We have performed comparative studies on the crystallinity of STO thin films with different deposition pressure, substrate temperature, and laser repetition rate. It seems that the quality of the STO thin films depends on the details of growth conditions, such as oxygen pressure, deposition rate, and substrate temperature. For example, the deposition temperature was found to be critical in obtaining single (100)-oriented STO thin films. Deposition at below 550 °C resulted in amorphous film; no RHEED and x-ray diffraction (XRD) pattern were observed. Growth at temperature above 690 °C, however, layer-by-layer sublimation from GaAs was found.<sup>13</sup>

XRD was employed to examine the in-plane and out-of-plane relationships between the STO thin film and GaAs substrate. Figure 2(a) displays a typical x-ray  $\theta$ - $2\theta$  diffraction pattern of a 3000 Å thick STO layer on GaAs. Only diffraction peaks of STO (001) and (002) were observed. This suggests that the as-grown films are a single (001) phase oriented. Both STO and GaAs have cubic unit cells, and the

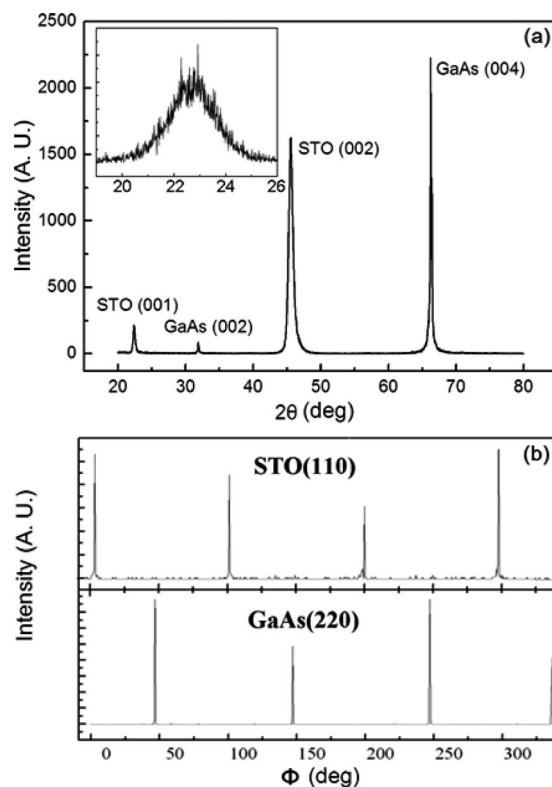


FIG. 2. XRD of STO/GaAs heterostructure. (a)  $\theta$ - $2\theta$  scan. The inset indicates the rocking curve for STO; (b)  $\Phi$  scan.

lattice constant is  $a_{\text{STO}}=0.3905$  nm and  $a_{\text{GaAs}}=0.565$  nm, respectively. For STO (001) parallel to the (001) of GaAs, the lattice mismatch is  $(|\alpha_{\text{STO}}-\alpha_{\text{GaAs}}|/\alpha_{\text{GaAs}})\times 100\%=31\%$ . This value is considerably large for a good epitaxial film growth. However, the mismatch would be relatively small for a 45° in-plane rotation of STO with respect to GaAs, i.e.,  $(|\sqrt{2}\alpha_{\text{STO}}-\alpha_{\text{GaAs}}|/\alpha_{\text{GaAs}})\times 100\%=2.2\%$ . The XRD 360°- $\varphi$  scan results confirm the heteroepitaxial relationship between STO and GaAs. The 45° in-plane rotation between STO and GaAs is evident, as seen in Fig. 2(b). The interface strain induced by lattice mismatch is gradually relaxed as the film thickness increases. Calculations based on the parameters from Fig. 2(a) yield lattice constants of 0.390 and 0.565 nm for the STO film and the GaAs substrate, respectively. Thus the STO film has a lattice parameter very close to the bulk material. Although the measurement is for out-of-plane lattice only, it nevertheless reflects that the strain of the STO film has relaxed at the film thickness. Rocking curve measurement of the STO film in the inset of Fig. 2(a) showed a full width at half maximum (FWHM) value of 1.6°. This somewhat large FWHM value is the result of the degraded crystallinity of the STO thin films grown on lattice mismatched (100)-oriented GaAs substrates via a 45° in-plane rotation.

As a potential template for integration functional perovskite oxide with GaAs, the surface morphology of the STO layer is of a major concern. We use atomic force microscopy (AFM) to study the surface of the STO/GaAs heterostructure. Figure 3 shows the surface morphology of STO films grown on GaAs. The as-grown film has very smooth surface

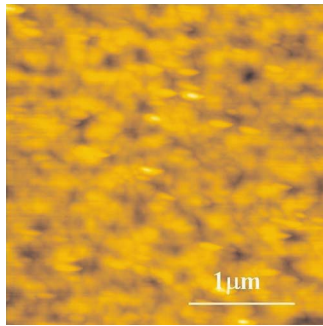


FIG. 3. (Color online) AFM images of the surface of 300 nm STO thin films grown on GaAs substrate.

with a root-mean square roughness values of 0.84 nm. Such good surface smoothness is attributed to the result of layer-by-layer growth mode shown in Fig. 1.

Figure 4 shows the variation of dielectric properties of the STO film as a function of frequency at room temperature. It is known that the bulk dielectric constant of STO was approximately 300. As shown in Fig. 4, the experimental dielectric constant value of STO film was smaller compared to that of STO bulk and decreased at increased frequency. The dielectric loss of the film was less than 0.02 for all values of measured frequency. According to Figs. 1(b) and 1(c), an in-plane rotation of STO has occurred. This reduced dielectric constant at room temperature may be attributed to the effect of GaAs as the bottom electrode and/or charge

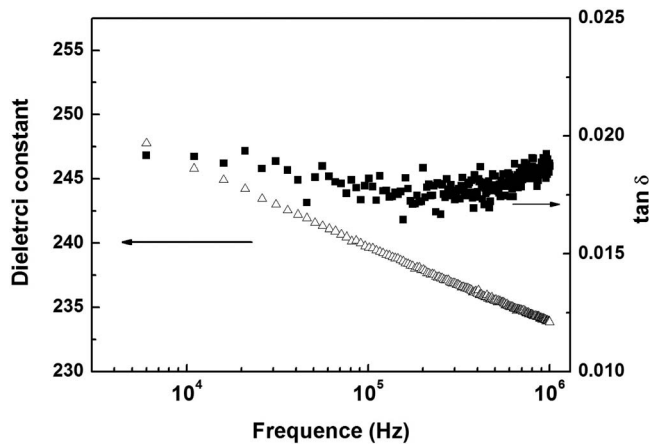


FIG. 4. Dielectric constant and loss of 300 nm STO film as a function of frequency at room temperature.

dissipation at oxide/semiconductor interface. Similar result was found in other researchers' work.<sup>14</sup> Based on STO/GaAs heterostructure, ferroelectric BaTiO<sub>3</sub> films have been fabricated on GaAs using STO as a buffer layer. The microstructure and ferroelectric properties of this ferroelectric/semiconductor heterostructure have been systematically studied. Details of those studies will be published elsewhere.

#### IV. CONCLUSIONS

In conclusion, epitaxial STO thin films have been successfully grown on GaAs substrates by LMBE. The in-plane orientation relationship with substrate is STO[110]||GaAs[001]. The surface morphology of films, as observed by AFM, was quite smooth. The dielectric characteristics of STO/GaAs heterojunction were also studied.

#### ACKNOWLEDGMENT

This work was supported by a grant from the Research Grants Council of Hong Kong (GRF Project No. PolyU7025/05P).

- <sup>1</sup>M. Hong, J. Kwo, A. R. Kortan, J. P. Mannaerts, and A. M. Sergent, *Science* **283**, 1897 (1999).
- <sup>2</sup>R. A. McKee, F. J. Walker, M. B. Nardelli, W. A. Shelton, and G. M. Stocks, *Science* **300**, 1726 (2003).
- <sup>3</sup>X. X. Xi, H. C. Li, W. Si, A. A. Sirenko, I. A. Akimov, J. R. Fox, A. M. Clark, and J. Hao, *J. Electroceram.* **4**, 393 (2000).
- <sup>4</sup>W. Chang, S. W. Kirchoefer, J. A. Bellotti, S. B. Qadri, and J. M. Pond, *J. Appl. Phys.* **98**, 024107 (2005).
- <sup>5</sup>C. Ang, L. E. Cross, Z. Yu, R. Guo, A. S. Bhalla, and J. H. Hao, *Appl. Phys. Lett.* **78**, 2754 (2001).
- <sup>6</sup>J. S. Wu, C. L. Jia, K. Urban, J. H. Hao, and X. X. Xi, *J. Mater. Res.* **16**, 3443 (2001).
- <sup>7</sup>J. H. Hao, J. Gao, Z. Wang, and D. P. Yu, *Appl. Phys. Lett.* **87**, 131908 (2005).
- <sup>8</sup>H. Li, X. Hu, Y. Wei, Z. Yu, X. Zhang, R. Droopad, A. A. Demkov, J. Edwards, Jr., K. Moore, W. Ooms, J. Kulik, and P. Fejes, *J. Appl. Phys.* **93**, 4521 (2003).
- <sup>9</sup>R. A. McKee, F. Walker, and M. Chisholm, *Phys. Rev. Lett.* **81**, 3014 (1998).
- <sup>10</sup>C. M. Wolfe, G. E. Stillman, and W. T. Lindley, *J. Appl. Phys.* **41**, 3088 (1970).
- <sup>11</sup>Y. Liang, J. Curless, and D. McCready, *Appl. Phys. Lett.* **86**, 082905 (2005).
- <sup>12</sup>Y. Liang, J. Kulik, T. C. Eschrich, R. Droopad, Z. Yu, and P. Maniar, *Appl. Phys. Lett.* **85**, 1217 (2004).
- <sup>13</sup>M. Ishida, S. Tsuji, K. Kimura, H. Matsunami, and T. Tanaka, *J. Cryst. Growth* **45**, 393 (1978).
- <sup>14</sup>Y.-Z. Yoo, P. Ahmet, Z. W. Jin, K. Nakajima, T. Chikyow, M. Kawasaki, Y. Konishi, Y. Yonezawa, J. H. Song, and H. Koinuma, *Appl. Phys. Lett.* **82**, 4125 (2003).